Desalination and Water Treatment
www.deswater.com

doi: 10.1080/19443994.2015.1098806

57 (2016) 23147–23161
October

Taylor & Francis
Taylor & Francis Group

Removal of scale-forming ions by a novel cation-exchange electrochemical system—A review

David Hasson*, Hilla Shemer, Raphael Semiat

Rabin Desalination Laboratory, Technion-Israel Institute of Technology, Haifa 32000, Israel, Tel. +972 4 8292936; Fax: +972 4 8295672; email: hasson@tx.technion.ac.il (D. Hasson)

Received 12 April 2015; Accepted 13 August 2015

ABSTRACT

Electrochemical removal of scale-forming ions from hard water is based on the generation of a high-pH environment around the cathode. Although the possibility of electrochemical scale removal has long been recognized, industrial application of this technique is rather restricted. Limitations of the conventional electroprecipitation technology are the high cathode area requirement, the existence of a limiting current density beyond which the precipitation rate remains unchanged and the cumbersome need for periodic cleaning of the cathode surface. A novel electrochemical technique overcomes the above limitations. In conventional equipment, the cathode performs two functions: it generates alkalinity on the boundary layer in immediate contact with the electrode and also serves as a scale deposition surface. The basic concept of the electrochemical cation-exchange system (ECM system) is locating the anode and cathode in two cells separated by a cation-exchange membrane. In this case, a high-alkaline environment is generated throughout the whole volume of the cathode compartment. By transferring the alkaline solution to a separate crystallization vessel containing seeds of the precipitating species, the crystal deposition surface is now the extensive area of the seeds rather than the restricted area of the cathode. The aim of the present paper is to review performance data and capabilities of the ECM technology. The order of magnitude reduction in cathode area requirement is illustrated by $CaCO_3$ scale precipitation data. Further improvement of the ECM technology by integration of bipolar membranes is shown to provide higher energy efficiencies and to enable complete prevention of the undesirable process of chlorine generation. Application of the ECM technique for phosphate removal from secondary treatment effluent containing calcium and magnesium hardness is described. Finally, the ECM technique is shown to have a high potential for the removal of heavy metals from industrial wastewaters.

Keywords: Electrochemical precipitation; Electrode area; Scale control; Phosphate removal; Heavy metals removal

---

*Corresponding author.

Presented at EuroMed 2015: Desalination for Clean Water and Energy Palermo, Italy, 10–14 May 2015. Organized by the European Desalination Society.

1. Introduction

Scale deposition is a difficulty-facing process in which aqueous solutions containing ions of sparingly soluble salts are heated, evaporated or concentrated. The problem is widely encountered in cooling tower systems and in both thermal and membrane desalination systems. Electrochemical scale removal offers many advantages: environmental compatibility, no need to handle and dose chemicals, accessibility to automation and convenient process control [1,2]. The possibility of alkaline scale precipitation and removal by electrochemical techniques has long been recognized. The basic mechanism involved is generation of a high-pH environment around the cathode by the following cathodic reactions:

$$2H_2O + 2e^- \rightarrow H_2\uparrow + 2OH^- \tag{1}$$

$$O_2 + 2H_2O + 4e^- \rightarrow 4OH^- \quad \text{(main cathodic reaction)} \tag{2}$$

The alkaline environment promotes precipitation of the calcium hardness in the form of $CaCO_3$ and magnesium hardness in the form of $Mg(OH)_2$ according to the following reactions:

$$Ca^{2+} + HCO_3^- + OH^- \rightarrow CaCO_3\downarrow + H_2O \tag{3}$$

$$Mg^{2+} + 2OH^- \rightarrow Mg(OH)_2\downarrow \tag{4}$$

The main anodic reactions are chlorine and oxygen gas evolutions:

$$2Cl^- \rightarrow Cl_2\uparrow + 2e^- \tag{5}$$

$$2H_2O \longrightarrow 4H^+ + O_2 + 2e^- \tag{6}$$

Despite the commercial availability of such equipment, the use of electrochemical scale control methods is limited to cooling towers and has not been applied to desalination systems. Three major limitations of the currently available technology are the high cathode area requirement, the need of periodical cleaning of cathode surface and the existence of a limiting current density beyond which the precipitation rate remains unchanged. Due to mass transfer limitations, an asymptotic precipitation rate level is reached at a current density in the range of 10–45 A/m^2 [3].

The high electrode area restriction can be illustrated by the following calculation: in a brackish desalination plant having a yearly output of Mm^3, the flow rate of the concentrate stream could be of the order 20 m/h. Assuming that the calcium content of the concentrate is around 2,000 mg/L as $CaCO_3$ and that it is desired to reduce this value by one-half in order to extract additional permeate, it is necessary to precipitate 20 kg/h $CaCO_3$. A typical precipitation rate attained with the current technology is around 50 g $CaCO_3$/h per m^2 cathode area. Thus, the required cathode area is as high as 400 m^2.

A novel electrochemical cell design (Fig. 1) overcomes the limitations of current electrochemical systems [4,5]. In the conventional equipment currently used for hardness reduction in cooling tower systems, the water is in contact with both the cathode and the anode electrodes. The cathode performs two functions: it generates alkalinity and serves as a scale deposition surface. The precipitation reaction occurs only in the water film adjacent to the cathodic surface where hydroxyl ions are generated, while the bulk of the water substantially retains the feed pH level.

The novel system adopts the scheme used in industrial production of NaOH. The anode and cathode are placed in disconnected compartments separated by a cationic ion-exchange membrane (Fig. 1). In this case, a high-alkaline environment is generated throughout the whole volume of the cathodic compartment and not only in the boundary layer adjacent

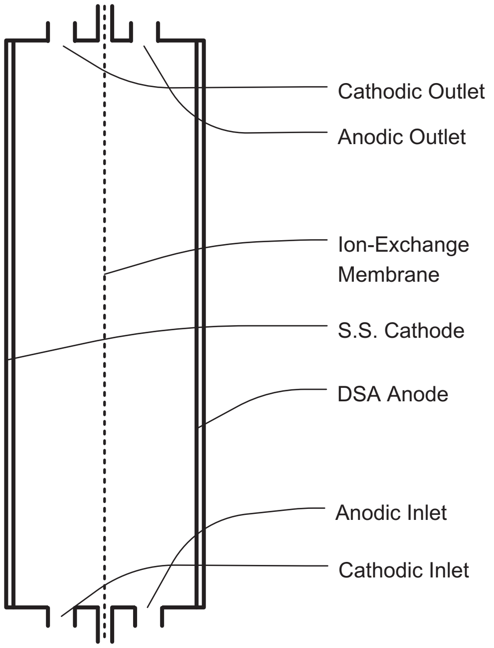

Fig. 1. Electrochemical cell with separate anodic and cathodic compartments.

to the cathode. In the anodic compartment, the gas generation reactions (5) and (6) occur leading to the transfer of cations to the cathodic compartment.

Significant enhancement of the $CaCO_3$ rate of precipitation is achieved by transferring the alkaline solution emanating from the cathodic compartment into a separate reaction vessel containing a suspension of calcium carbonate seeds (Fig. 2). The seeds offer an extensive precipitation area, in contrast to the restricted area available in a system relying on the cathode to provide a crystallization surface. Moreover, use of seeds rather than the cathode to serve as the scale deposition surface overcomes the difficulty of disposal of scale adhering on the cathode. As shown below, the improved system enables an order of magnitude reduction of the cathode area.

The objective of this paper is to review data characterizing the capabilities of the electrochemical membrane (ECM) technology for the removal of undesirable ionic species.

2. Cathode area reduction in alkaline scale precipitation

Data below illustrate the significant cathode area reduction that can be achieved with the ECM system in comparison with the performance of a conventional electrochemical scale precipitation (ESP) system. The electrolytic cell of the conventional system consisted of a stainless steel tube having an internal diameter of 56 mm serving as a cathode and a central titanium rod of 25 mm diameter serving as a dimensionally stable anode [6]. Calcium carbonate scale deposition on the cathode was measured with NaCl solutions of 35 mS/cm conductivity containing a total alkalinity of 38 meq/L and a calcium concentration of either 12 or 24 mmol/L. The inlet pH was 7.6.

Calcium carbonate precipitation results of the ECM system were obtained from the set-up shown in Fig. 2 with two different ECM cells: a relatively high electrical resistance of 900-mL cell enabling operation up to a current density of 120 A/m^2 and a relatively low resistance 50-mL cell enabling operation up to a current density of 600 A/m^2. Feed solutions had a calcium concentration in the range of 4–8 mmol/L and total alkalinity in the range of 5–10 meq/L. Solution conductivity was around 7.5 mS/cm and inlet pH was in the range of 6.8–8.1.

Figs. 3 and 4 display the results comparing precipitation rates obtained by the ESP and the ECM systems. It is seen that with the conventional ESP system, an asymptotic limit is reached when attempting to increase the precipitation rate by augmenting the current density. No such limit is present in the ECM system—precipitation rate increases linearly with current density. Precipitation rates above 1,200 g/h m^2 electrode area were obtained with the low-resistance ECM system compared to less than 100 g/h m^2 with the conventional ESP system.

The specific energy requirement depends on the cell resistance and the solution composition. Fig. 5 displays the effect of calcium concentration on the specific energy consumption in the precipitation of $CaCO_3$ in the 50-mL electrochemical cell at a constant current density of 600 A/m^2 and a constant feed flow rate of

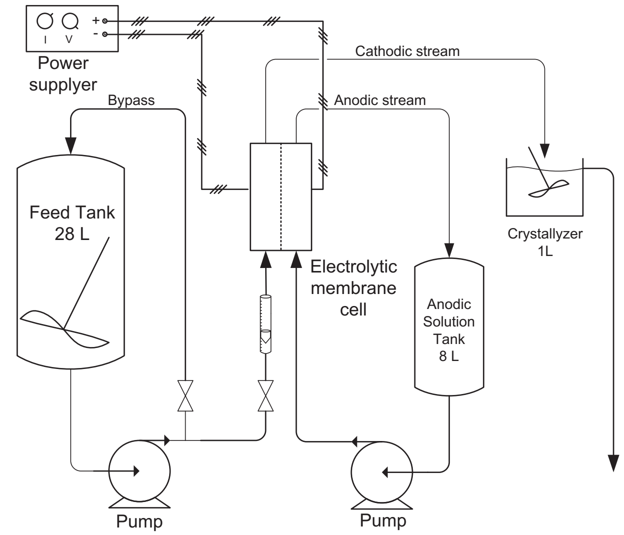

Fig. 2. Flow sheet of the ECM precipitation system.

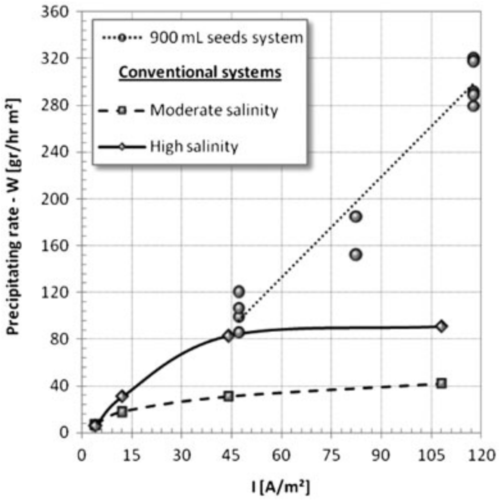

Fig. 3. $CaCO_3$ precipitation in the high-resistance 900-mL cell compared with data measured in conventional ESP systems.

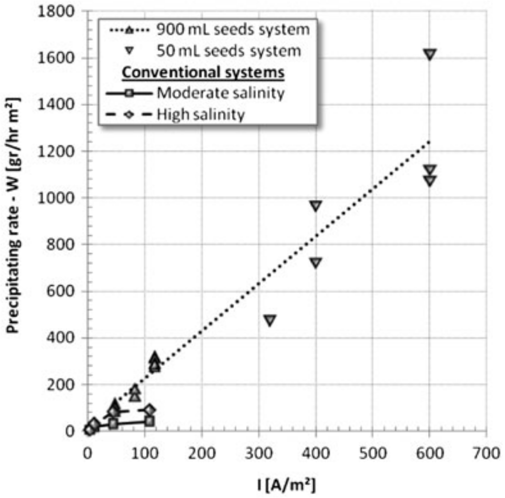

Fig. 4. $CaCO_3$ precipitation in the ECM systems compared with data measured in conventional ESP systems.

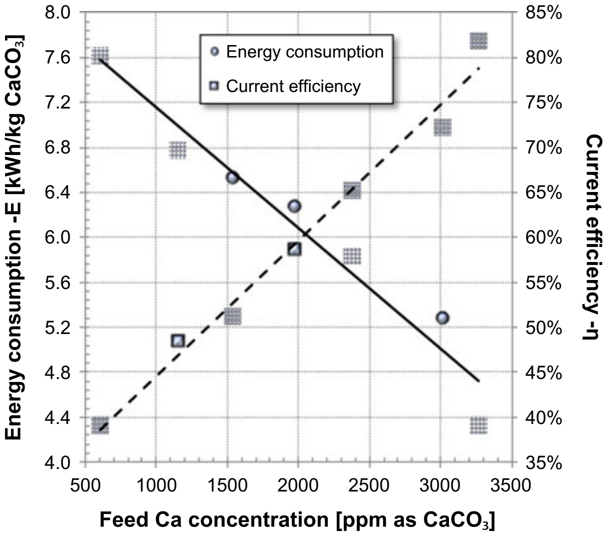

Fig. 5. Effect of calcium feed concentration on the energy consumption and the current efficiency.

70 mL/min. The feed solution was maintained at the pH of 6.4 and the molar ratio of calcium to alkalinity was held at 1.6.

It is seen that the energy consumption is in a reasonable range of 4–8 kW h per kg $CaCO_3$. Current efficiency expresses the ratio of OH^- ions consumed in the precipitation of $CaCO_3$ and in the increase of solution alkalinity to the theoretical OH^- ions generated by the electric current. Energy consumption is lowered and current efficiency is augmented at increasing the feed solution concentrations.

3. Improved $CaCO_3$ precipitation with a bipolar membrane system

All current electrochemical scale removal systems release chlorine at the anode, as shown in Eqs. (5) and (6). The ECM system was further improved by integration of bipolar membranes (BM) [7]. Inclusion of BM enables complete prevention of the undesirable process of chlorine generation at the anode. Moreover, it enables higher current efficiencies and Faraday yields at reduced energy consumptions.

A bipolar membrane (Fig. 6) consists of a negatively charged cationic membrane glued to a positively charged anionic membrane. When placed in an electrolytic cell with the cation side facing the cathode and the anion side facing the anode, cations and anions are unable to transfer the electric current. This induces the water molecules to split into H^+ and OH^- ions, so as to transfer the current [8,9]. As seen in Fig. 6, the end result is acidity near the cathode and alkalinity near the anode. If the solution contains NaCl, this salt will decompose to the acid and base that formed this salt.

3.1. Verification of BM energy reduction

Verification of the energy reduction provided by the electrochemical cell with bipolar membrane (EBM) was carried out in the system, shown in Fig. 7, consisting of one bipolar membrane interposed between two cation-exchange membranes (CEM). Feed solution was used as anode rinse solution. In this case (denoted as configuration A), chlorine generation is not prevented. Table 1 displays the composition of the tested solutions which simulated seawater and brackish water, respectively. Table 2 displays the operating conditions

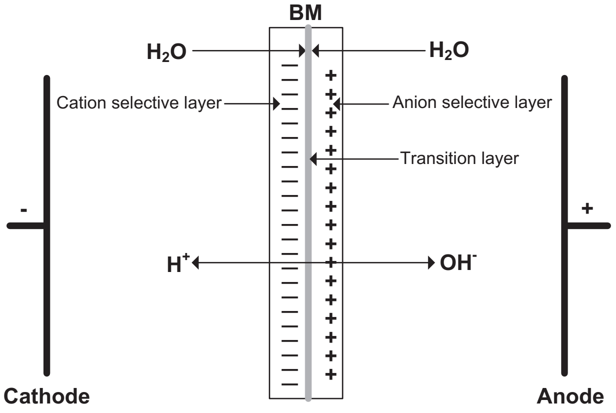

Fig. 6. Bipolar membrane structure and water splitting in transition region.

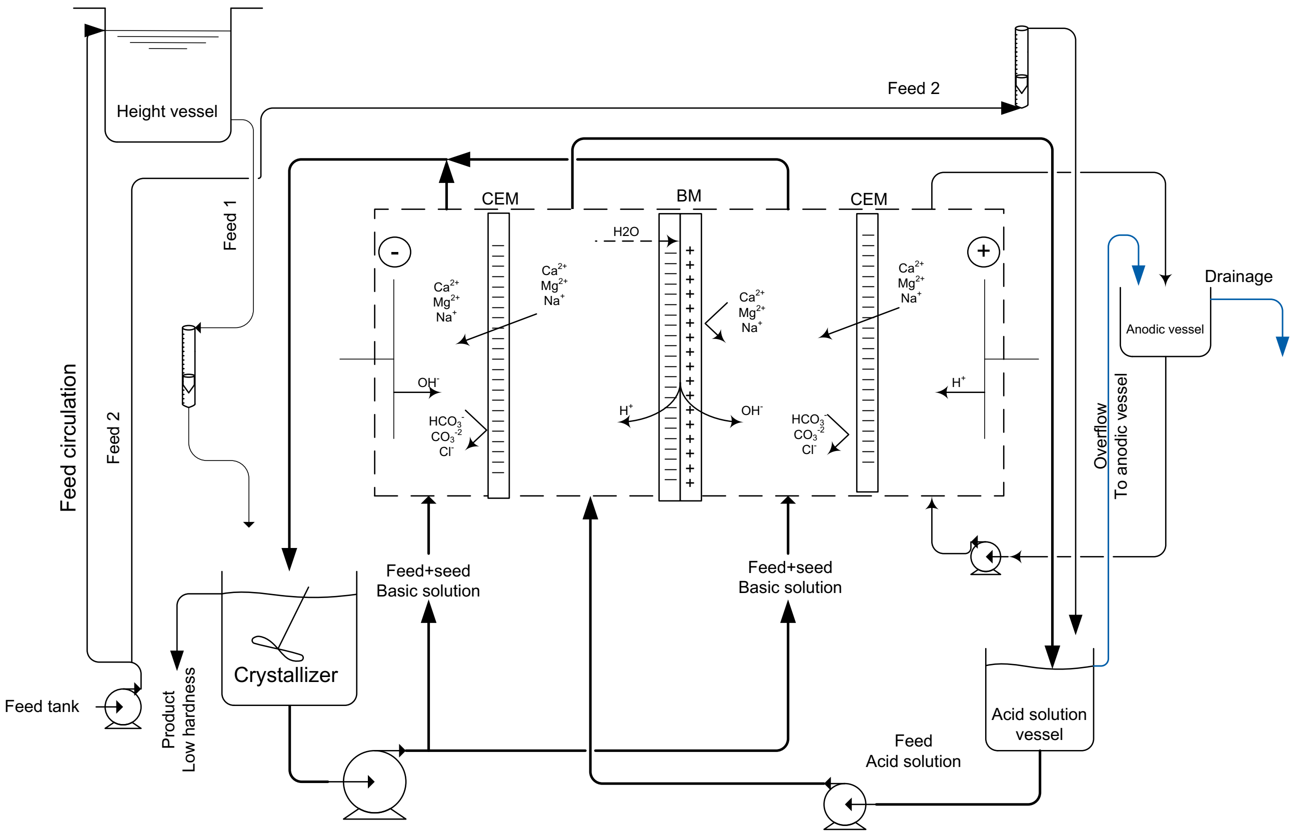

Fig. 7. Electrochemical system with a bipolar membrane interposed between two CEM membranes (configuration A).

Table 1
Composition of solutions used in the EBM efficiency tests

Component	Seawater concentration (M)	Brackish water concentration (M)
Ca^{2+}	0.0106	0.016
Na^{+}	0.4861	0.062
Mg^{2+}	0.0548	–
Cl^{-}	0.5657	0.090
HCO_3^{-}	0.0018	0.006
pH	8.1	6.5–7

of the EBM system which are seen to be closely similar to those used in the comparable ECM experiments. In the seawater experiments, CO_2 gas was bubbled into the intermediate-sealed vessel, feeding the crystallizer.

Results shown in Table 3 confirm the superior performance of the bipolar system over the ECM system. The EBM system is seen to enable a higher $CaCO_3$ hardness removal at lower current densities and energy consumptions. Also, values of the current efficiency in the bipolar membrane system are seen to be higher than those in the ECM system and in one instance, the EBM efficiency is higher than 100%.

Current efficiencies in bipolar cells can exceed 100% due to processes that take place in a bipolar membrane [7]. At a current efficiency above 100%, the mass of $CaCO_3$ removed is higher than the mass of the OH^- produced by the cathode reactions evaluated

Table 2
Operating conditions of the EBM system

Solution	Feed flow rate (L/h)	Electric current (A)	Current density (A/m^2)	CO_2 flow rate (mL/min)	Crystallizer resid. time (min)	Temperature (℃)
Brackish water	10	2–3	100–150	–	60	20–26
Seawater	10	5–7	250–350	60–70	60	20–26

Table 3
Comparison of the EBM and ECM systems' performance in $CaCO_3$ precipitation

Solution	System	Current density (A/m^2)	Voltage ΔV (V)	Crystal. pH	Precipitation rate (g/h m^2)	Energy consumption (kW h/kg $CaCO_3$)	Current efficiency, φ (%)
Brackish water	ECM	150	5.8	7.7	350–400	2.2	74–82
	EBM	100	7.7	10.7	460	1.7	110
Seawater	ECM	350	8.2	9–9.3	525–575	5.0–6.0	53–55
	EBM	250	6.7	8.8–9	530–570	2.8–3.0	72–85

Table 4
Comparison of current density requirements by the EBM and the ECM systems for similar $CaCO_3$ precipitation rates in brackish water

System	Current density (A/m^2)	Voltage, ΔV (V)	Crystal. pH	Precipitation rate (g/h m^2)	Energy consumption (kW h/kg $CaCO_3$)	Current efficiency, φ (%)
ECM	100	4.1	7.2	280	1.5	95
	150	4.6	7.4	520	1.4	98
EBM	100	7.6	7.5	630	1.2	139

by Faraday's law. The generated hydroxyl ions are removed from solution by direct reaction with carbonate species leading to water splitting in the BM membrane. Another source generating hydroxyl ions is the extra water dissociation process occurring at the solution–membrane interface due to boundary layer concentration polarization.

Table 4 shows the results of experiments comparing the current intensities required for achieving a similar degree of $CaCO_3$ removal from brackish water in the two systems. A current of 2 A (100 A/m^2) was sufficient in the EBM system to obtain the high precipitation rate of 630 g/h/m^2, while a current of 3 A (150 A/m^2) was required in the ECM system to reach a precipitation rate of 520 g/h/m^2. The energy consumed in $CaCO_3$ removal in the ECM system was higher than that in the EBM system. It is therefore clearly evident that hardness removal by the EBM system occurs at a higher current efficiency and consumes less energy.

3.2. *EBM chlorine free system*

Chlorine evolution can be prevented by avoiding contact of the feed solution with the anode. This was accomplished using external 0.1 M Na_2SO_4 solutions to rinse the electrodes rather than rinsing the electrodes by the feed solution.

Two configurations were tested: configuration C (Fig. 8) in which a single bipolar membrane was interposed between two CEM and configuration D (Fig. 9) in which a single cation-exchange membrane was interposed between two BM. The performance of these systems was tested using the brackish water solution of Table 1.

Table 5 displays the results of the $CaCO_3$ removal in the three flow configurations of the EBM system. It is seen that the performance of the chlorine free systems was similar to that of the chlorine-generating system; the use of external Na_2SO_4 solution for electrode rinse did not influence the effectiveness of the $CaCO_3$ removal process. Current efficiency was very high in the three tested EBM systems.

4. ECM removal of phosphate ions from treated wastewater

Municipal wastewaters may contain 5 to 20 mg/L total phosphorous, of which 1–5 mg/L is organic and the rest is inorganic [10,11]. Removal of phosphate from wastewaters can serve three important functions: recovery of phosphorous for its value as a chemical commodity, preventing environmental problems associated with algae growth in surface water and phosphate removal from secondary-treated wastewaters to enable scale-free membrane purification which provide irrigation quality water.

A difficulty presently hindering wider reuse of wastewater reclamation for unrestricted irrigation purposes is the lack of a reliable anti-scalant for preventing calcium phosphate precipitation in reverse osmosis or nanofiltration tertiary treatments. The

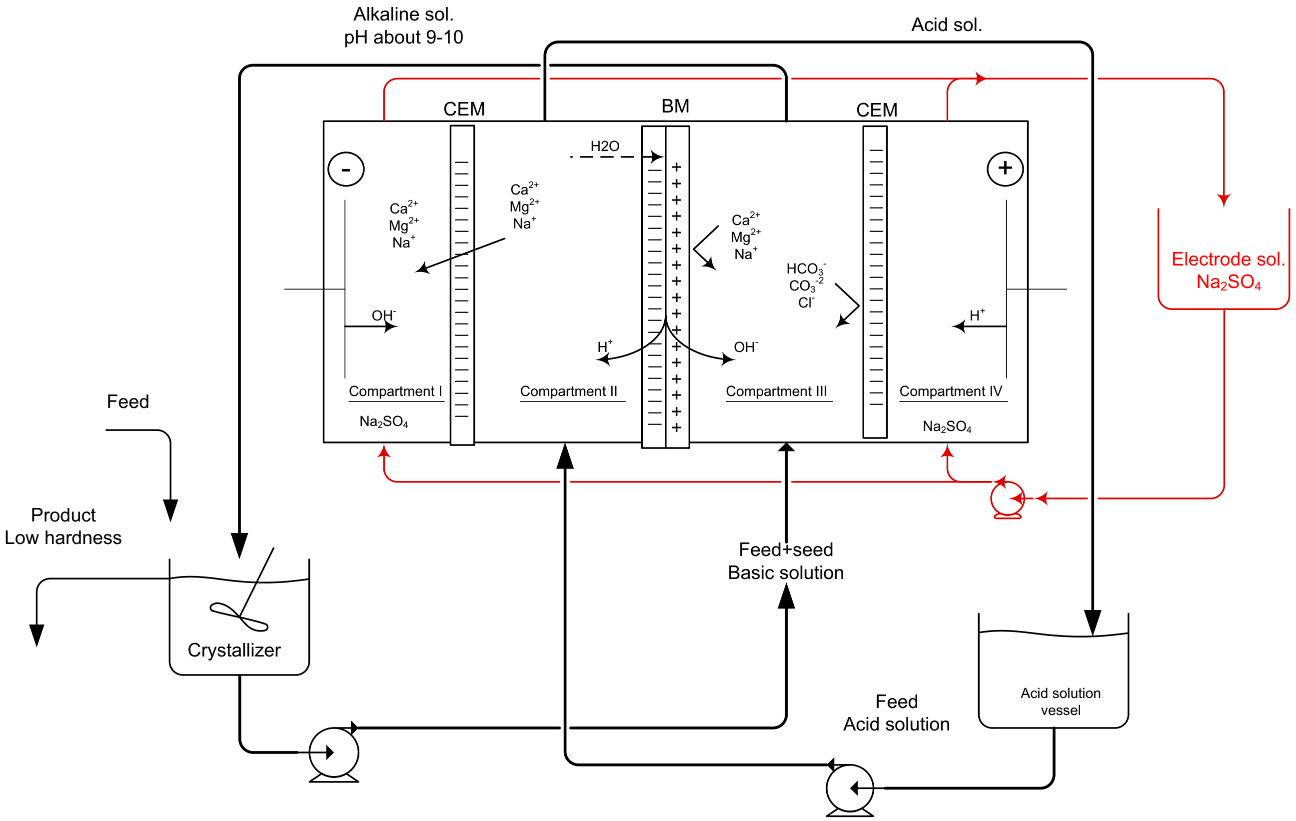

Fig. 8. Chlorine-free bipolar experimental system with flow configuration C.

potential of the ECM system for beneficial removal of phosphate together with $CaCO_3$ and $Mg(OH)_2$ from a secondary effluent was characterized [12] using a feed solution simulating the composition of an Israeli domestic wastewater treatment plant which is shown in Table 6.

The ECM system was operated with either a 50-mL cell or a 300-mL cell with a flow sheet similar to that shown in Fig. 2. The inlet feed flow rate was 100 mL/min. The crystallizer was operated at a retention time of 100 min and at a pH controlled in the range of 9.5–11.5. The alkaline solution created in the electrochemical cell induced precipitation of most of the calcium ion as $CaCO_3$, the magnesium ion as $Mg(OH)_2$ and the phosphate ion as hydroxyapatite [$Ca_5(PO_4)_3(OH)$].

4.1. Effect of current density on the precipitation

Fig. 10 shows the effect of current density on the total precipitation rate of the three species ($CaCO_3$, $Mg(OH)_2$ and $Ca_5(PO_4)_3(OH)$). It is seen that the precipitation rate increases linearly with the current density over the whole range investigated (100–350 A/m^2). This result is not possible to achieve with conventional ESP systems since, as mentioned in Section 1, the precipitation rate cannot be increased beyond an asymptotic limit occurring usually below 50 A/m^2.

Fig. 11 shows the effect of current density on the fractional removal of phosphate ions as well as on the residual phosphate concentration. It is seen that a minimum residual phosphate concentration of 1.2 mg/L was obtained at a current density of 360 A/m^2. The fractional removal of the phosphate ion was 70% at the current density of 100 A/m^2 and reached an asymptotic limit of 87% at the current density of 300 A/m^2.

4.2. Effect of pH on phosphate removal

The solubility of calcium phosphates decreases at increasing pH levels. A series of experiments were carried out with the two electrochemical cells to determine the residual phosphate concentration at different pH levels in the crystallizer. Static equilibrium solubility experiments were also carried out to measure phosphate solubility of the investigated solution at different pH levels. The static experiments were carried

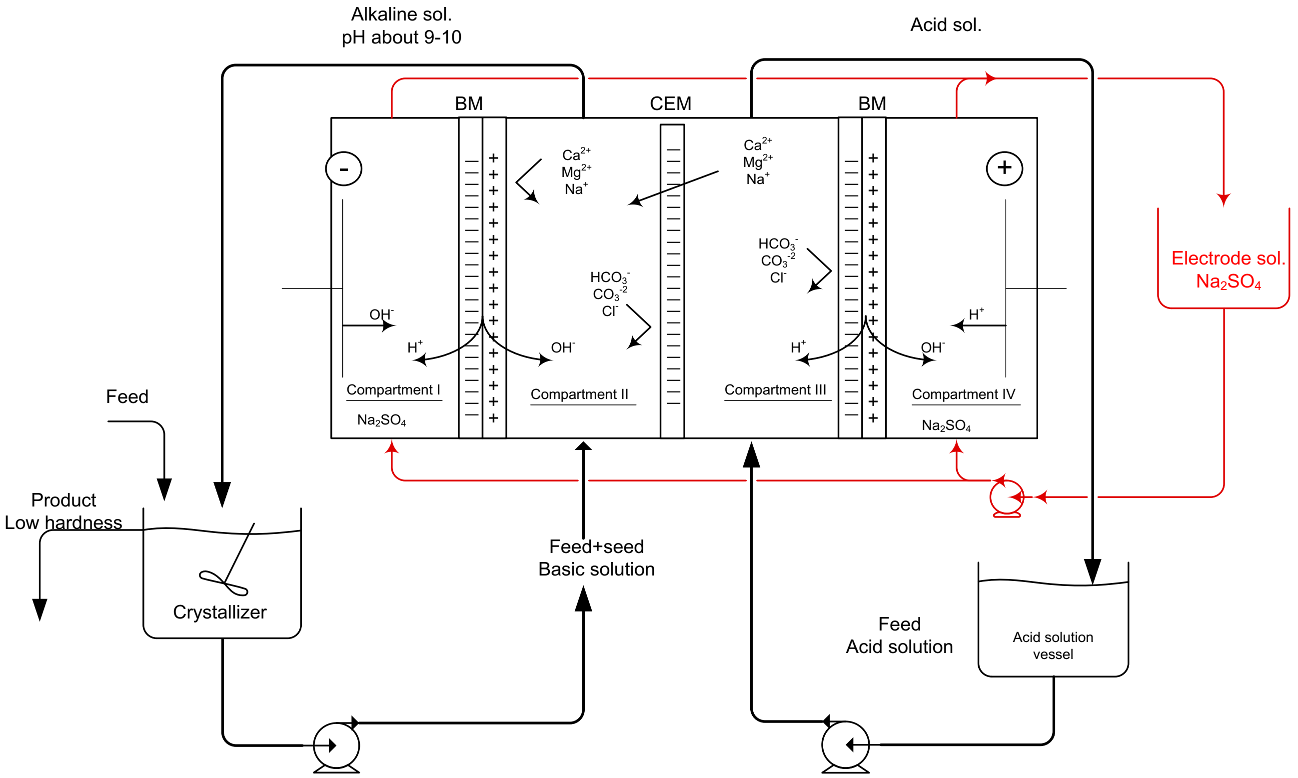

Fig. 9. Chlorine-free bipolar experimental system with flow configuration D.

Table 5
Performance of chlorine-free EBM systems (configurations C and D) with that of chlorine-generating EBM system configuration A

EBM configuration	Electrode rinse	Electric current (A/m^2)	Voltage ΔV (V)	Crystal. pH	Precipitation rate (g/h m^2)	Energy consumption (kW h/kg $CaCO_3$)	Current efficiency, φ (%)
A	Feed	100	7.6	7.5	630	1.2	139
C	Na_2SO_4 0.1 M	200	8.8	8.3	685–776	2.3–2.5	99–108
D	Na_2SO_4 0.1 M	100	7.0	7.5	530	1.3	131
		200	11	8.4	781	2.8	109

out using a 250-mL sealed Erlenmeyer flask held in a water bath at 25˚C and agitated for 24 h at 200 rpm.

Fig. 12 displays residual phosphate concentrations determined from both the continuous flow electrochemical experiments and from the equilibrium solubility data measured in the static flask experiments. The continuous flow residual phosphate data are seen to be very close to the equilibrium solubility measurements. This indicates that the residence time of the solution in the crystallizer (100 min) was sufficient to provide phosphate precipitation very close to equilibrium. Fig. 12 indicates that a residual phosphate of less than 1 mg/L can be achieved by maintaining a pH of 10.5 in the crystallizer.

4.3. Effect of phosphate ions on the precipitation rate of alkaline scale species

Effective anti-scalants are based on organic and inorganic polymeric phosphates. Even nonpolymeric inorganic phosphates can moderately inhibit the precipitation of $CaCO_3$ and $Mg(OH)_2$ [13]. The influence of the presence of phosphate ions on the course of alkaline scales precipitation was tested by comparing

Table 6
Composition of feed solution used in phosphate removal tests

Component	(mg/L)
PO_4^{3-}	9.9
Cl^-	341.0
Ca^{2+}	85.6
Mg^{2+}	34.2
Na^+	210.0
SO_4^{2-}	82.4
Alkalinity (mg/L as $CaCO_3$)	284.1
Turbidity (NTU)	0.3
Conductivity (μS)	1,740
pH	7.0

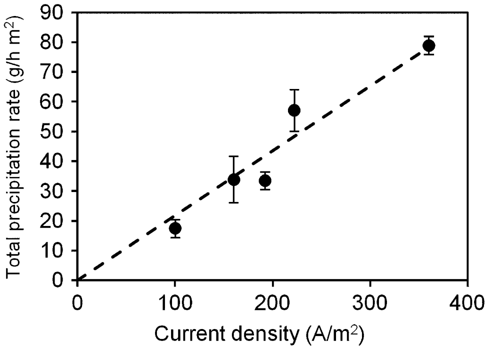

Fig. 10. Effect of current density on the total precipitation rate.

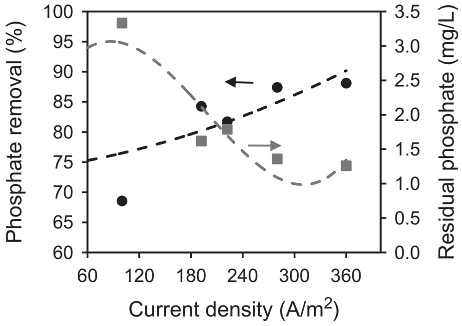

Fig. 11. Effect of current density on the phosphate removal and the residual phosphate.

the precipitation degree at different pH levels in the crystallizer with and without the presence of phosphate ions.

Figs. 13 and 14 display the removal level of calcium and magnesium at increasing values of the pH induced by augmenting the current density. The data clearly show that the presence of phosphate acts to reduce the precipitation level of both $CaCO_3$ and $Mg(OH)_2$.

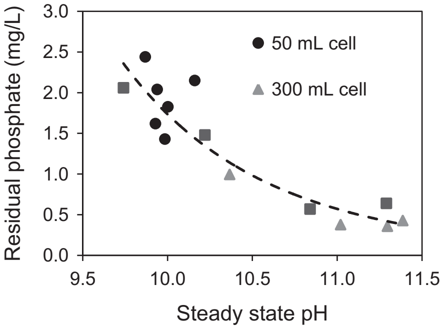

Fig. 12. Effect of pH on the residual phosphate concentration.

Further evidence on the inhibitory effect of phosphate ions on precipitation of the alkaline species was obtained by determining the fractional removal of the various species (phosphate, calcium and magnesium) as a function of time in all pH experiments. The data shown in Fig. 15 for the experiment preformed at a pH of 11.0 illustrate a phenomenon observed in all pH experiments. Calcium phosphate was found to be the first precipitating species. Only when most of the phosphate was removed, calcium carbonate started to precipitate. Magnesium was the last precipitating species.

The practical implication of the above results is that the presence of phosphate ions in hard water moderates the precipitation of alkaline scale species.

4.4. Energy consumption and current efficiency

Energy consumption in an electrochemical system depends on several parameters, notably distance between electrodes, electrodes overpotential and solution conductivity. Current efficiency is lowered by unwanted processes such as ion leakage through the membrane and undesired side reactions.

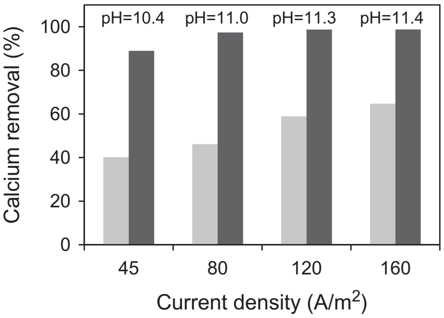

Fig. 13. Effect of current density on calcium removal in the absence (black) and in the presence (grey) of phosphate ions.

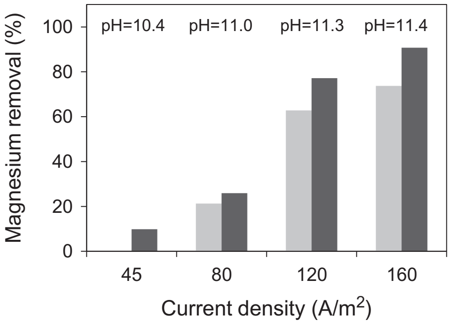

Fig. 14. Effect of current density on magnesium removal in the absence (black) and in the presence (grey) of phosphate ions.

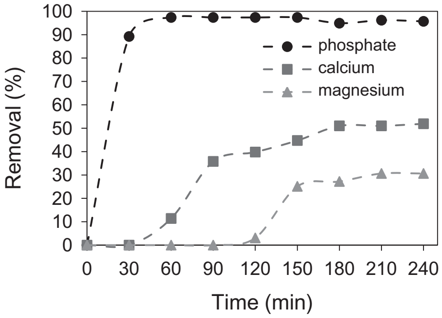

Fig. 15. Sequence of phosphate, calcium and magnesium precipitations at pH 11.0.

Table 7 summarizes results of the specific energy consumption and the current efficiency obtained with the various cells. It is seen that in most experiments, current efficiencies were high exceeding 85%. The specific energy consumption in the various experiments ranged from 0.5 to 3 kW h per m^3. From a practical point of view, the specific energy for a viable electrochemical phosphate removal process should be less than 0.5–1 kW h/m^3. Such conditions were realized in some of the experiments carried out here with simple laboratory equipment. It is reasonable to assume that an electrochemical cell of optimum design would enable phosphate removal meeting economic criteria.

In summary, the results indicate feasibility of viable electrochemical phosphate removal by the convenient ECM technique.

5. ECM removal of heavy metal ions from industrial wastewaters

5.1. Heavy metals removal techniques

The presence of heavy metal contaminants in wastewater stems from the increasing usage of heavy metals in industrial processes. Industrial discharges generate heavy metal concentrations far exceeding the low levels encountered in natural environments. For example, the concentrations of the main metallic contaminants of the plating industry (zinc, chromium, copper, cadmium and nickel) may reach levels as high as 1,000 mg/L [14–17].

Unlike organic contaminants, heavy metals are not biodegradable and tend to accumulate in living organisms. Most countries are increasingly placing restrictive regulatory limits on the concentration of metals that may be discharged either directly to the environment or to a wastewater treatment plant. The increasing volumes of heavy metal discharges are prompting efforts directed to improve current processes and to develop more effective treatment techniques.

Although a variety of techniques are available for the removal of heavy metal pollutants, difficulties are often encountered in practical applications due to various interferences and process limitations. Chemical precipitation of heavy metals is by far the most widely used process due to its relative simplicity [18–20]. The most widely used technique is hydroxide precipitation achieved by treating the wastewater with NaOH or $Ca(OH)_2$.

Electrochemical treatment is a promising technology. It has the significant advantages of simple equipment, convenient operation and non-requirement of chemical substances. A variety of electrochemical techniques have been used for treating wastewaters containing heavy metals including electrowinning [21], electrodialysis [22], electroflotation [23] and electrocoagulation [16].

5.2. ECM removal of copper and zinc

The capabilities of the ECM system for heavy metal ions removal were examined using copper and zinc solutions. The precipitation of these ions is induced by the high-pH environment generated in the cathodic cell enabling hydroxide precipitation in the crystallization vessel:

$$Cu^{2+} + 2OH^- \rightarrow Cu(OH)_2 \downarrow \qquad (7)$$

$$Zn^{2+} + 2OH^- \rightarrow Zn(OH)_2 \downarrow \qquad (8)$$

Metal hydroxides precipitation is notably influenced by solution pH levels. Cowan and Weintritt [13] reported that the lowest solubility of $Cu(OH)_2$ and $Zn(OH)_2$ occurs at pH values of 7.0–7.5 and 8.0–8.5, respectively. However, hydroxide solubility based on GWB-Geochemist's Workbench software [24] gives

Table 7
Energy consumption and current efficiency in phosphate precipitation

Cell	Current density (A/m^2)	Voltage ΔV (V)	Crystallizer pH	PO_4 removal (%)	Rate of total precipitation (g/ h m^2)	Energy consumption (kW h/kg $CaCO_3$)	Current efficiency (%)
50 mL	160	10.3	9.8	77.6	41.6	0.7	89.2
	192	11.7	9.9	84.3	33.5	0.9	87.4
	222	13.6	10.2	81.7	64.2	1.3	99.6
	360	12.3	9.9	88.1	78.9	1.8	76.4
300 mL	45	5.0	10.4	91.3	13.3	0.7	88.6
	80	5.9	11.0	96.3	14.9	1.6	98.1
	120	7.5	11.3	96.5	18.5	2.9	89.3

somewhat different pH values: 9.0–10.5 for Cu and 8.5–11.5 for Zn.

Heavy metal removal experiments were performed with the ECM system of Fig. 2 using the 300-mL cell. The fresh feed solution was supplied to the crystallizer and anodic vessel at the flow rate of 10 L/h, providing a solution retention time of 1 h. The crystallizer and anodic solutions were recirculated through the cathode and anode compartments at flow rates of about 10 L/min, respectively.

5.2.1. ECM system performance

The ECM system performance was examined by the removal of copper and zinc present in solution either alone (“separate” solution) or together (“composite” solution). The heavy metal ions concentration was 50–60 mg/L and the solution contained 8 g/L NaCl leading to a conductivity of about 12.5 mS/cm, which is in the range of wastewater conductivities of 8–75 mS/cm reported in the literature [15,25,26]. The feed solution pH was maintained at a value of about 5. Experimental conditions are summarized in Table 8.

Figs. 16 and 17 show that precipitation of heavy metals can be achieved in the ECM system at a very high degree of removal exceeding 99% at current efficiencies of 70–80%.

5.2.2. Effect of initial metal ion concentration

Faraday’s law predicts that the required current intensity for total removal of a metal ion is proportional to its feed concentration, leading to commensurate the higher precipitation rates and energy consumptions. This prediction was tested in runs performed with copper ions tap water solutions. Flow rate and residence time were as in the previous runs (Table 8). Table 9 confirms that removal of 99% of copper from a doubled initial solution concentration at doubled current intensity provides an almost doubled precipitation rate and energy consumption.

5.2.3. Effect of initial pH of feed solution

Industrial wastewaters commonly have an acidic pH range of 1–4. The effect of feed pH on the ECM performance was investigated with composite solutions of Zn and Cu at initial pH values of 2.5, 3.5 and 5.5 (Table 10) and the flow conditions listed in Table 8. As anticipated, in order to remove above 99% of the metal, the higher the feed acidity, the higher the required current density and the more elevated is the energy consumption.

5.2.4. Effect of solution composition

The presence of calcium and carbonate ions can influence the heavy metal removal, since the carbonate system affects the buffer capacity of a solution. Carbonate species such as H_2CO_3 and HCO_3^- consume hydroxyl ions produced at the cathode. This leads to a requirement of a more elevated current density for achieving a high metal removal. In addition, simultaneous calcium carbonate precipitation is known to promote heavy metal precipitation [27].

The effect of calcium carbonate presence in precipitating a heavy metal was studied by carrying out heavy metal removal experiments in the presence and absence of calcium and carbonate ions. Tests were carried out with both separate solutions of copper and composite solutions of zinc and copper. The solutions were prepared by dissolution of the corresponding salts in DI water containing 8 g/L NaCl. The experimental conditions are shown in Table 11.

Table 8
Conditions in the copper and zinc removal experiments at a crystallizer residence time of 60 min

Metals concentration (mg/L)	Feed flow rate (L/h)	Feed pH	Current density (A/m^2)	Crystallizer pH
Cu-50	10	5.5	25	10.0–10.2
Zn-65	10	5.5	35	10.2–10.5
Zn-55; Cu-60	10	5.5	65	10.6–10.7

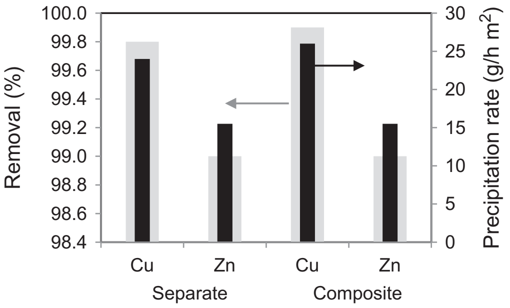

Fig. 16. Zinc and copper removal extent and precipitation rate in separate and composite solutions.

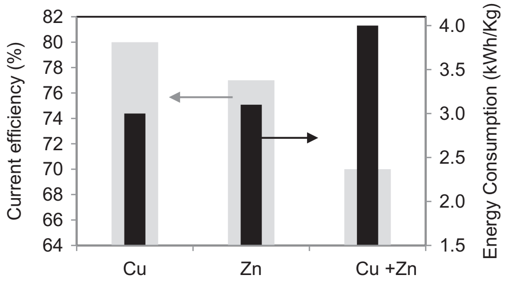

Fig. 17. Energy consumption and current efficiency for Cu and Zn precipitation in separate and composite solutions.

Table 12 compares copper precipitation results without and with calcium carbonate precipitation. It is seen that at a current density of 25 A/m^2, the high removal level of 99.8% achieved in the absence of calcium carbonate was reduced to 88% by hydroxyl-consuming calcium carbonate system. It was possible to recover a high copper removal level of 98.7% by providing double current intensity of 50 A/m^2 which required an increase in the energy demand from 3 to 6.7 kW h/kg.

Table 13 compares copper and zinc precipitation results without and with calcium carbonate precipitation. It is seen that at the current density of 65 A/m^2, high removal levels above 99% were achieved for both metals in the absence of calcium carbonate. To achieve comparable removal levels in the presence of calcium carbonate system, it was necessary to increase the current intensity to 200 A/m^2 leading to an increase in the energy demand from 4.0 to 12.3 kW h/kg. It may be concluded that ECM heavy metals removal in the presence of the calcium carbonate system requires operation at adequately increased current intensities.

5.2.5. Comparison of ECM performance with other heavy metals electrolytic systems

Tables 14 and 15 provide data enabling comparison of the performance of ECM system in heavy metal removal with that of other electrolytic techniques. Table 14 summarizes the data on specific energy consumption and specific removal rates reported in relevant literature studies, while Table 15 summarizes the results obtained in the various experimental series of the present study.

The specific energy consumption data of the ECM system are seen to be significantly lower than those of other systems. Yet, pending further work, it is uncertain whether this result is an inherent advantage of the ECM system or is due to the lower concentration levels of the solutions tested in the ECM system. However, the comparison of specific removal rates of the ECM system with those of other electrolytic

Table 9
Copper removal at different initial feed concentrations at pH 5.0

Current efficiency (%)	Energy consumption (kW h/kg)	Total removal (%)	Precipitation rate (g/h m^2)	Current density (A/m^2)	Feed concentration (mg/L)
64	4.3	99.2	30.5	40	62
64	10.6	99.5	57.3	75	116

Table 10
Precipitation of Zn and Cu at different levels of the feed solution

Metal concentration (mg/L)	Feed pH	Current density (A/m^2)	Precipitation rate (g/h m^2)	Total removal (%)	Energy consumption (kW h/kg)
Zn-58	2.5	150	29	99.6	11.8
Cu-54			27	100	
Zn-60	3.5	78	26	99	4.9
Cu-53			30	99.3	
Zn-58	5.5	65	29	99	4.0
Cu-53			26	99.9	

Table 11
Experimental conditions in heavy metal removal from solutions containing calcium and carbonate ions

Solution composition (mg/L)	Feed pH	Calcite saturation (LSI)	Feed flow rate (L/h)	Current density (A/m^2)	Crystallizer retention time (min)
Cu 50 Ca 330 Talk 160 as $CaCO_3$	5.5	−2.5	10	25–50	60
Zn 60 Cu 50 Ca 320 Talk 150 as $CaCO_3$	5.5	−2.5	10	200	60

Table 12
Copper precipitation from a solution containing calcium and carbonate ions

Solution composition (mg/L)	Feed pH	Current density (A/m^2)	Total removal (%)	Precipitation rate (g/h m^2)	Energy consumption (kW h/kg)	Current efficiency (%)
Cu 50	5	25	99.8	24.0	3.0	80
Cu 50 Ca330 Talk 160 as $CaCO_3$	5	25	88.0	21.4	3.3	91
Cu 50 Ca 330 Talk 160 as $CaCO_3$	5	50	98.7	23.9	6.7	71

Table 13
Copper and zinc precipitation from a solution containing calcium and carbonate ions at pH 5

Solution composition (mg/L)	Current density (A/m^2)	Metals removal (%)	Precipitation rate (g/h m^2)	Energy consumption (kW h/kg)	Current efficiency (%)
Zn 58 Cu 53	65	99.8	24.0	3.0	70
Zn 60 Cu 50 Ca 330	200	Zn 99.0	Zn 29	4	78
Talk 160 as $CaCO_3$		Cu 99.9	Cu 26		

techniques shows an unambiguous clear advantage to the ECM technique.

Literature data on total operating costs in electrochemical processes of heavy metal removal indicate values in the range of 5–7 US\$/m^3 of treated solution [16,25,28–31]. Electrical energy costs contributed 5–20% to the total cost, i.e. 0.3 and 2.3 US \$/m^3 (0.11–3 US\$/kg). Results of the ECM system show much lower electrical energy costs of about 0.02–0.05 US\$/m^3 (0.4–0.5 US\$/kg).

In summary, the ECM system enables total removal of heavy metal ions. Values of the specific energy costs and specific removal rates measured in this study indicate a potential for beneficial

Table 14
The literature values of specific energy consumption and overall removal rate

Solution concentration (mg/L)	Removal method	Energy consumption (kW h/k)	Precipitation rate (mol/h m^2)	Refs.
Cu^{2+} 932 Cr^{6+} 964 Ni^{2+} 468	ED	42.3	0.14	Hunsom et al. [25]
Cu^{2+} 250	ED	–	0.46	Llanos et al. [28]
Ni^{2+} 376 Cu^{2+} 283 Zn^{2+} 75 Cr^{6+} 167	EC	45.6	0.76	Dermentzis et al. [16]
Zn^{2+} 500 Cu^{2+} 500	EC	70	0.40	Nouri et al. [29]

Table 15
Specific energy consumption and overall removal rates of the ECM system

Data of section	Solution concentration (mg/L)	Feed pH	Current density (A/m^2)	Precipitation rate (mol/h m^2)	Energy consumption (kWh/kg)	Metals recovery (%)
5.2.1	Cu 50 Zn 50	5.5	25–65	0.85	3.0–4.0	99.0–99.9
5.2.2	Cu 62–116	5.0	40–75	0.48–0.49	4.0–11	99.2–99.5
5.2.3	Cu 50 Zn 50	2.5–5.5	65–150	0.87	4.0–12	99.0–99.9
5.2.4	Cu 50 (Talk 160 Ca 330)	5.0	25–50	0.34–0.38	3.0–7.0	88–98.7
5.2.4	Cu 50 Zn 60 (Talk 150 Ca 320)	5.5	200	0.84	12	99.4%

application of zinc and copper removal by the ECM system. The value of recovered heavy metals can yield an additional beneficial effect to the treatment costs. The prices of copper and zinc exceed 8,000 and 2,000 US$ per ton, respectively. Results of this study show that separation of 50 mg/L of Cu and 50 mg/L of Zn can be achieved with an electrical energy consumption of 3–4 kW h/kg at an estimated cost of less than 500 US$ per ton.

6. Concluding remarks

Bench-scale laboratory data on various process separations reported in this review and ongoing research results on additional processes indicate a significant potential for the beneficial application of ECM systems in desalination and wastewater purification applications. Available information justifies the verification of laboratory results on a pilot plant scale.

Acknowledgement

This paper is based on studies performed with the participation of the following researchers: O. Gorni-Pinkesfeld, G. Greenberg, V. Lumelsky, Y. Pinhas and I. Zaslavschi. Thanks to the Israel Water Authority for sponsoring a part of the work.

References

[1] L.J.J. Janssen, L. Koene, The role of electrochemistry and electrochemical technology in environmental protection, Chem. Eng. J. 85 (2002) 137–146.
[2] K. Rajeshwar, G. Ibanez, G.M. Swain, Electrochemistry and the environment, J. Appl. Electrochem. 24 (1994) 1077–1091.
[3] C. Gabrielli, G. Maurin, H. Francy-Chausson, P. Thery, T.T.M. Tran, M. Tlili, Electrochemical water softening: Principle and application, Desalination 201 (2006) 150–163.
[4] D. Hasson, G. Sidorenko, R. Semiat, Calcium carbonate hardness removal by a novel electrochemical seeds system, Desalination 263 (2010) 285–289.

[5] D. Hasson, G. Sidorenko, R. Semiat, Low electrode area electrochemical scale removal system, Desalin. Water Treat. 31 (2011) 35–41.

[6] D. Hasson, V. Lumelsky, G. Greenberg, Y. Pinhas, R. Semiat, Development of the electrochemical scale removal technique for desalination applications, Desalination 230 (2008) 329–342.

[7] I. Zaslavschi, H. Shemer, D. Hasson, R. Semiat, Electrochemical $CaCO_3$ scale removal with a bipolar membrane system, J. Membr. Sci. 445 (2013) 88–95.

[8] H. Strathmann, J.J. Krol, H.J. Rapp, G. Eigenberger, Limiting current density and water dissociation in bipolar membranes, J. Membr. Sci. 125 (1997) 123–142.

[9] A.J.B. Kemperman (Ed.), Handbook on Bipolar Membrane Technology, first ed., Twente University Press, The Netherlands, 2000.

[10] M. Özacar, Contact time optimization of two-stage batch adsorber design using second-order kinetic model for the adsorption of phosphate onto alunite, J. Hazard. Mater. 137 (2006) 218–225.

[11] N.Y. Mezenner, A. Bensmaili, Kinetics and thermodynamic study of phosphate adsorption on iron hydroxide-eggshell waste, Chem. Eng. J. 147 (2009) 87–96.

[12] O. Gorni-Pinkesfeld, H. Shemer, D. Hasson, R. Semiat, Electrochemical removal of phosphate ions from treated wastewater, Ind. Eng. Chem. Res. 52 (2013) 13795–13800.

[13] J.C. Cowan, D.J. Weintritt, Water-Formed Scale Deposits, Gulf Publishing Co., Houston, TX, 1976.

[14] S.I. Amer, Treating Metal Finishing Wastewater. Available from: <http://www.pfonline.com/articles/treating-plating-wastewater>, Accessed September, 2015.

[15] G. Srisuwan, P. Thongchai, Removal of heavy metals from electroplating wastewater by membrane, Songklanakarin J. Sci. Technol. 24 (2002) 965–976.

[16] K. Dermentzis, A. Christoforidis, E. Valsamidou, Removal of nickel, copper, zinc and chromium from synthetic and industrial wastewater by electrocoagulation, Int. J. Environ. Sci. 5 (2011) 697–710.

[17] M.P.S. Khurana, P. Singh, Waste water use in crop production: A review, Resour. Environ. 2 (2012) 116–131.

[18] X. Lin, R.C. Burns, G.A. Lawrance, Heavy metals in wastewater: The effect of electrolyte composition on the precipitation of cadmium(II) using lime and magnesia, Water Air Soil Pollut. 165 (2005) 131–152.

[19] S.A. Mirbagheri, S.N. Hosseini, Pilot plant investigation on petrochemical wastewater treatment for the removal of copper and chromium with the objective of reuse, Desalination 171 (2004) 85–93.

[20] B. Chen, R. Qu, J. Shi, D. Li, Z. Wei, X. Yang, Z. Wang, Heavy metal and phosphorus removal from waters by optimizing use of calcium hydroxide and risk assessment, Environ. Pollut. 1 (2012) 38–54.

[21] V. Stankovic, Metal removal from effluents by electrowinning and a new design concept in wastewater purification technology, Chem. Biochem. Eng. Q 21 (2007) 33–45.

[22] R.F.D. Costa, C.W. Klein, A.M. Bernardes, J.Z. Ferreira, Evaluation of the electrodialysis process for the treatment of metal finishing wastewater, J. Braz. Chem. Soc. 13(4) (2002) 540–547.

[23] A.K. Chopra, A.K. Sharma, V. Kumar, Overview of electrolytic treatment: An alternative technology for purification of wastewater, Arch. Appl. Sci. Res. 3(5) (2011) 191–206.

[24] C.M Bethke, S. Yeakel, GWB Essentials Guide–Release 8.0, 2008, 116 pp.

[25] M. Hunsom, K. Pruksathorn, S. Damronglerd, H. Vergnes, P. Duverneuil, Electrochemical treatment of heavy metals (Cu^{2+}, Cr^{6+}, Ni^{2+}) from industrial effluent and modeling of copper reduction, Water Res. 39 (2005) 610–616.

[26] I. Heidmann, W. Calmano, Removal of Zn(II), Cu(II), Ni(II), Ag(I) and Cr(VI) present in aqueous solutions by aluminium electrocoagulation, J. Hazard. Mater. 152 (2008) 934–941.

[27] A. Khelifa, S. Moulay, A.W. Naceur, Treatment of metal finishing effluents by the electroflotation technique, Desalination 181 (2005) 27–33.

[28] J. Llanos, R. Camarillo, A. Pérez, P. Canizares, M.A. Rodrigo, Costs estimation of an integrated process for the treatment of heavy-metal loaded aqueous effluents, J. Appl. Electrochem. 41 (2011) 1099–1107.

[29] J. Nouri, A.H. Mahvi, E. Bazrafshan, Application of electrocoagulation process in removal of zinc and copper from aqueous solutions by aluminum electrodes, Int. J. Environ. Res. 4(2) (2010) 201–208.

[30] S. Chellammal, S. Raghu, P. Kalaiselvi, G. Subramanian, Electrolytic recovery of dilute copper from a mixed industrial effluent of high strength COD, J. Hazard. Mater. 180 (2010) 91–97.

[31] N. Kongsricharoern, C. Polprasert, Electrochemical precipitation of chromium (Cr) from an electroplating wastewater, Water Sci. Technol. 31 (1995) 109–117.